Peptides 59 (2014) 42–52

Contents lists available at ScienceDirect

Peptides

journal homepage: www.elsevier.com/locate/peptides

Hyperalgesic and edematogenic effects of Secapin-2, a peptide isolated from Africanized honeybee (*Apis mellifera*) venom

D. Mourelle[a], P. Brigatte[a], L.D.B. Bringanti[a], B.M. De Souza[a], H.A. Arcuri[a], P.C. Gomes[a], N.B. Baptista-Saidemberg[b], J. Ruggiero Neto[c], M.S. Palma[a,*]

[a] CEIS/Dept. Biology, Institute of Biosciences of Rio Claro, São Paulo State University (UNESP), Rio Claro, SP, Brazil
[b] Department of Anatomy, Cell Biology and Physiology and Biophysics, Institute of Biology, State University of Campinas, Brazil
[c] Department of Physics/IBILCE, São Paulo State University (UNESP), São José do Rio Prêto, SP, Brazil

ARTICLE INFO

Article history:
Received 16 June 2014
Received in revised form 1 July 2014
Accepted 2 July 2014
Available online 11 July 2014

Keywords:
Hyperalgesia
Inflammation
Honeybee venom
Secapin
Peptidomics

ABSTRACT

Honeybee stings are a severe public health problem. Bee venom contains a series of active components, including enzymes, peptides, and biogenic amines. The local reactions observed after envenoming include a typical inflammatory response and pain. Honeybee venom contains some well-known polycationic peptides, such as Melittin, Apamin, MCD peptide, Cardiopep, and Tertiapin. Secapin in honeybee venom was described 38 years ago, yet almost nothing is known about its action. A novel, variant form of this peptide was isolated from the venom of Africanized honeybees (*Apis mellifera*). This novel peptide, named Secapin-2, is 25 amino acid residues long. Conformational analyses using circular dichroism and molecular dynamics simulations revealed a secondary structure rich in strands and turns, stabilized by an intramolecular disulfide bridge. Biological assays indicated that Secapin-2 did not induce hemolysis, mast cell degranulation or chemotactic activities. However, Secapin-2 caused potent dose-related hyperalgesic and edematogenic responses in experimental animals. To evaluate the roles of prostanoids and lipid mediators in the hyperalgesia and edema induced by this peptide, Indomethacin and Zileuton were used to inhibit the cyclooxygenase and lipoxygenase pathways, respectively. The results showed that Zileuton partially blocked the hyperalgesia induced by Secapin-2 and decreased the edematogenic response. In contrast, Indomethacin did not interfere with these phenomena. Zafirlukast, a leukotriene receptor antagonist, blocked the Secapin-2 induced hyperalgesia and edematogenic response. These results indicate that Secapin-2 induces inflammation and pain through the lipoxygenase pathway in both phenomena.

Introduction

The venoms of the social Hymenoptera are complex mixtures of biologically active compounds, such as low molecular mass compounds, peptides, and proteins [17,39]. Peptide toxins usually constitute up to 70% of the composition of these venoms. It is well known that insect stings on human skin can induce ongoing pain, hyperalgesia (and allodynia), and inflammation [10,11]. However, the mechanisms underlying these responses are poorly studied.

These peptides seem to induce a series of pharmacological actions that are observed during envenoming caused by honeybee, wasp and ant stings [39]. These actions generally result in a series of envenoming processes, such as generalized inflammation, intravascular hemolysis with increased bilirubin levels, decreased levels of haptoglobin, hemoglobinuria and thrombocytopenia, disseminated intravascular coagulation, rhabdomyolysis, increased levels of creatine kinase and aldolase, and acute tubular necrosis, among others [22,23,29]. These actions complicate the establishment of a proper diagnosis and the choice of a suitable clinical strategy to overcome the envenoming effects [14,17].

The chemical diversity of the peptides in Hymenoptera venoms, have been exploited by using a combination of techniques such as high-performance liquid chromatography (HPLC) and mass spectrometry have been applied to aid the discovery of novel components of social wasp venoms. For example, this analytical approach led to the detection of more than 100 different peptides in the venom of the wasp *Polybia paulista* [19]. In the wasps' venom, different types of inflammatory peptides such as mastoparans, protonectin-like peptides, chemotactic peptides, and kinins were identified [16,31,39]. Additionally, in honeybee venoms, the peptide components already reported include Melittin [38] and its

* Corresponding author at: CEIS/IBRC-UNESP, Avenue 24-A 1515, Bela Vista, 13506-900 Rio Claro, SP, Brazil. Tel.: +55 19 35264163; fax: +55 19 35264163.
E-mail address: mspalma@rc.unesp.br (M.S. Palma).

http://dx.doi.org/10.1016/j.peptides.2014.07.004
0196-9781/

analogs [3,24], Apamin [45,46], mast cell degranulating (MCD) peptide [7], Cardiopep [47], Tertiapin [50] and Secapin [25,28], as well as a few others that have been studied.

Secapin is a polycationic peptide with 25 amino acid residues that contains an intramolecular disulfide bridge; it represents approximately 0.5% of the dry weight of honeybee venom [3,39]. This peptide was originally reported in the venom of an European honeybee (*Apis mellifera*) race without clear identification of the subspecies [24]; the sequence of this peptide was completely assigned later by two independent groups [35,49]. However, these studies did not investigate the biological actions of Secapin. Recently, a novel, variant form of Secapin was described in the venom of *A. mellifera* in China without any functional characterization [37]. Until now, this peptide has apparently exhibited no toxicity in mammals because the administration of high doses (up to 80 mg/kg) had no lethal effects; at this dose, the animals were reported to exhibit only signs of sedation within the first 15 min of administration, followed by piloerection and hypothermia [24].

In the present study, a novel form of Secapin that was isolated from the venom of Africanized honeybees is reported; therefore, the aim of this work was the structural and functional characterization of this novel form, termed Secapin-2, focusing on the induction of hyperalgesic and edematogenic effects, as well as on the mechanisms involved in these phenomena.

Material and methods

Animals

Male Swiss mice, weighing between 25 and 30 g, were used throughout this study. The mice were housed under controlled humidity at a temperature of 22 ± 1 °C and subjected to a 12 h light–dark cycle in a sound-attenuated room. Food and water were available ad libitum, and the mice were taken to the testing room at least 1 day before the experiment. All behavioral testing was performed between 9:00 am and 4:00 pm. Each mouse was used only once. All experiments were in accordance with the guidelines for the ethical use of conscious animals in pain research, published by the International Association for the Study of Pain [51]. The procedures were approved by the Institutional Animal Care Committee at São Paulo State University/UNESP campus Rio Claro/SP (CEUA-IB-UNESP-CRC, Protocol n° 1984). Efforts were made to minimize the number of animals used and their suffering.

Biological material

The venom from Africanized *A. mellifera* was obtained from the apiary at the Institute of Biosciences of Rio Claro – UNESP, at Rio Claro, SP, southeast Brazil; the venom was milked from the bees using a device that produces pulsed electric discharges at the entrance of the nest. The worker bees stimulated by these discharges stung a plastic film covering a glass plate that was positioned at the nest entrance, depositing small liquid droplets over the plates. The glass plates containing many droplets of the liquid venom were then dried under a flow of chilled air (4 °C), and the dried venom was scraped from the glass plate. The solid venom was then lyophilized, pooled, and stored at −80 °C until use.

Venom fractionation

The peptide fraction was obtained by suspending 5 mg of the crude venom from Africanized honeybees (*A. mellifera*) in 2 mL of 50% (v/v) acetonitrile (MeCN) with shaking for 15 min at 4 °C. The suspension was then centrifuged at 10,000 × *g* for 10 min at 4 °C. The supernatant was collected, pooled, and lyophilized, and the total peptide fraction was stored at −80 °C until use. The peptide fraction was then chromatographed on a Capcell Pack C-18 UG120 column (10 mm × 250 mm, 5 μm, Shisheido) under a linear gradient from 5 to 60% (v/v) MeCN/H_2O [containing 0.1% (v/v) trifluoroacetic acid (TFA)] at a flow rate of 2.0 mL/min for 60 min and monitored by UV absorption at 214 nm with a UV-DAD detector (Shimadzu, mod. SPD-M10A). The fractions were manually collected in glass vials and dried using a lyophilizer.

Amino acid sequencing

The amino acids were sequenced using a gas-phase sequencer PPSQ-21A (Shimadzu) based on automated Edman degradation chemistry.

Peptide synthesis

The peptides were prepared by stepwise, manual solid-phase synthesis using N-9-fluorophenylmethoxy-carbonyl (Fmoc) chemistry with Novasyn TGS resin (NOVABIOCHEM). The side-chain protective groups included t-butyl (tBu) for serine, t-butoxycarbonyl (Boc) for lysine, and β-t-butyl ester (OtBu) for aspartic acid. The side-chain protective group trityl (Trt) was used in the synthesis of the oxidized peptide (with the disulfide bridge). Cleavage of the peptide–resin complexes was performed by treatment with trifluoroacetic acid/1,2-ethanedithiol/anisole/phenol/water (82.5:2.5:5:5:5 by volume) at room temperature for 2 h. After filtering to remove the resin, anhydrous diethyl ether (Sigma) at 4 °C was added to the soluble material to cause precipitation of the crude peptide, which was collected as a pellet by centrifugation at 1000 × *g* for 15 min at room temperature. The crude peptide was solubilized in water and purified by RP-HPLC. The peptide with the disulfide bridge was obtained by air oxidation of the cysteine residues as described elsewhere [1].

The synthetic peptide was purified by high-performance liquid chromatography (HPLC, mod. LC 8A) using a Shim-Pack C-18 Prep-ODS (K) column (30 mm × 250 mm, 15 μm, Shimadzu) under isocratic elution with 45% (v/v) MeCN/H_2O [containing 0.05% (v/v) TFA] at a flow rate of 10 mL/min. The elution was monitored at 214 nm with a UV-Vis detector (Shimadzu, mod. SPD-20A Prominence). The fractions were manually collected and dried using a lyophilizer (Heto). The homogeneity and correctness of the sequence of the synthetic peptides were assessed using a gas-phase sequencer PPSQ-21A (Shimadzu) based on automated Edman degradation chemistry and ESI-MS analysis. The synthetic peptide was used in all the bioassay protocols.

Mass spectrometry

Mass spectrometric analyses were performed on an Ion Trap/Time-of-Flight hybrid mass spectrometer (LCMS-IT-TOF) produced by Shimadzu Co. (Kyoto, Japan). The samples were injected into the LC–MS system with an autosampler injector at a flow rate of 0.2 mL/min of 50% (v/v) MeCN. All analyses were performed in the positive electrospray ionization (ESI+) mode using typical conditions: a CDL temperature of 200 °C, a capillary voltage of 4.5 kV, a cone voltage of 3.5 V, a flow rate of the nebulizer gas (nitrogen) of approximately 1.5 L/h and a drying gas (nitrogen) flow rate of 100 L/h. The ESI mass spectra were obtained in the continuous acquisition mode, scanning from *m*/*z* 50 to 4000 for 2 min. The data were acquired and analyzed using LCMS solution software (SHIMADZU, Kyoto, Japan).

Circular dichroism measurements

To evaluate the conformational changes in the peptides induced by different membrane-mimetic environments, CD spectra were obtained at a peptide concentration of 20 μM in either bi-distilled water, 40% (v/v) 2,2,2-trifluoroethanol (TFE)/water, or sodium dodecyl sulfate solutions (SDS) above and below the critical micelle concentration (CMC) of SDS (8 mM and 165 μM SDS, respectively). The CD spectra were recorded from 260 to 190 nm with a Jasco-815 spectropolarimeter (JASCO International Co. Ltd., Tokyo, Japan) calibrated routinely at 209 nm using a D-pantolactone solution [30]. The spectra were acquired at 25 °C using a 0.5 cm path length cell at a scan speed of 20 nm/min, a bandwidth of 1.0 nm, a response of 0.5 s, and a resolution of 0.1 nm. Eight scans were acquired for each spectrum. Following a baseline correction, the observed ellipticity in θ (mdeg) was converted to mean residue ellipticity $[\Theta]$ (deg cm^2/dmol) using the relationship $[\Theta] = 100\theta/(l \times c \times n)$, where "*l*" is the path length in centimeters, "*c*" is the millimolar peptide concentration, and "*n*" is the number of peptidic bonds. Assuming a two-state model, the observed mean residue ellipticity at 222 nm ($\Theta^{obs}{}_{222}$) was converted into an α-helix fraction (f_H) using the method proposed by Rohl and Baldwin [40].

Molecular modeling

The search for templates of the Secapin sequence was performed with the short BLASTP algorithm [2], and the alignment was formatted and input into the program. The structure of the homologous peptide, which was experimentally solved by NMR (PDB ID: 2KRI) [13], was selected from the Protein Data Bank (PDB) [5]. Peptide models were built with restraint-based modeling implemented in MODELLER 9v11 [41] using the standard protocols for comparative protein structure modeling by the satisfaction of spatial restraints [36,43]. For each peptide, a total of 1000 models were created, and the best ones were selected according to the MODELLER objective function and stereochemical analysis using PROCHECK [34]. The sequence similarity between Secapin and the template was 43% (38% identity). The final models were selected with 90% of the residues in favored regions of the Ramachandran plot, with the best values for the overall *G*-factor and lower values of energy minimization. The oxidized form of Secapin was modeled; PyMOL was used for the visualization of the Secapin model [15].

Molecular dynamics simulations

The MD simulations were performed with the GROMACS 4.5.5 software package [48] using the GROMOS 43A1 force field [24] and the flexible SPC (Simple Point Charge) water mode [42]. For TFE molecules in the simulation, the model and simulation conditions were applied as proposed by Fioroni et al. [21]. The simulations of both peptides were carried out in a cubic box containing TFE and water corresponding approximately to a mixture of 40:60% (v/v) TFE:water in which the minimum distance between the peptide surface and the box face was 1.0 nm in all directions and neutralized with five Cl^- counter ions. During the simulations, the bond lengths within the peptides were constrained by the LINCS algorithm, and the SETTLE algorithm [27] was used to constrain the water geometry. In the initial MD simulation, Secapin and all the hydrogen atoms, ions, and water molecules were subjected to 500 steps of energy minimization by steepest descent to remove close van der Waals contacts. Both systems were then subjected to a short molecular dynamics simulation with position restraints for a period of 20,000 picoseconds (ps). The final MD simulations were performed under the same conditions, except that the position restraints were removed after an interval of 20,000 ps. The energy minimization and MD were carried out under periodic boundary conditions. The simulation was computed in the NPT ensemble at 300 K with Berendsen temperature coupling and a constant pressure of 1 atm with isotropic molecule-based scaling [4,12]. The temperature and pressure were modulated using coupling techniques [4] with coupling and isothermal compressibility constants of 0.01 ps (solvent and peptide) and 6.5×10^{-5} bar^{-1}, respectively. The electrostatic interactions between non-ligand atoms were evaluated by the particle mesh Ewald method [20]. The cut-off distances for the calculation of the Coulomb and van der Waals interactions were 1.0 and 1.4 nm, respectively. The convergences of the different simulations were analyzed in terms of the radius of gyration (RG), root mean-square deviation (RMSD) from the initial structures of the models, and types of intermolecular hydrogen bonds. All analyses were performed on the ensemble of system configurations extracted at 0.5 ps time intervals from the simulation, and the MD trajectory collection was initiated after 1 ns of dynamics to ensure a completely equilibrated evolution. The molecular visualization was performed in the graphical environment PyMOL.

Hemolytic activity

Washed rat red blood cells (WRRBC) were used to evaluate the hemolytic activity of the peptide. WRRBC were prepared by washing 50 mL of red blood cell suspensions from Wistar rats three times with physiological saline solution [0.85% (w/v) NaCl and 10 mM $CaCl_2$] and re-suspending them in 50 mL of the same solution. Aliquots of the WRRBC (0.5%, v/v) were then incubated at 37 °C in the presence of peptide for 120 min with gentle mixing. The samples were then centrifuged, and the absorbance of the supernatant was measured at 540 nm. The absorbance of lysed WRRBC incubated in 1% (v/v) Triton X-100 was considered to be 100%. The results are expressed as an average (±SD).

Mast cell degranulation activity

Mast cell degranulation was determined by measuring the release of β-D-glucosaminidase (co-localized with histamine) as modified by De Souza et al. [18]. Mast cells were obtained as a mixture of leukocytes by washing the peritoneum of adult Swiss mice with a solution containing 0.877 g NaCl, 0.028 g KCl, 0.043 g NaH_2PO_4, 0.048 g KH_2PO_4, 0.10 g glucose, 0.10 g BSA, 90 mL of a 2 M $CaCl_2$ solution, and 50 μL Liquemine (heparin, ROCHE) in 100 mL water. The mast cells were incubated in the presence of peptide for 15 min at 37 °C. After centrifugation, the supernatants were subjected to the β-D-glucosaminidase assay. Briefly, 50 μL of the mast cell suspension was added to 50 μL of the substrate [3 mg of p-nitrophenyl-N-acetyl-β-D-glucosaminidine (Sigma) dissolved in 10 μL of a 200 mM sodium citrate solution, pH 4.5] and incubated for 6 h at 37 °C. The reaction was stopped by the addition of 150 μL 0.2 M TRIS, pH 9.0, and the absorbance of the product was measured at 405 nm in a microtiter plate reader (Biotrack, Amersham Bioscience). The values were expressed as the percentage of total β-D-glucosaminidase, which was determined from lysed mast cells incubated with 0.1% (v/v) Triton X-100. The results were expressed as an average (±SD). Melittin was used as a standard compound for positive control of this assay.

Chemotactic activity

Chemotaxis was assayed in a specific multi-chamber apparatus (NeuroProbe, USA) using PMNL cells obtained from subcutaneous inflammatory induction in Swiss mice. A special membrane with 10 μm pores was introduced between the two parts of the chemotaxis apparatus, which allowed the migration of leucocytes. The total cell concentration was 10^5 cells/mL. The upper chambers were filled with 200 μL of PMNL suspension (2.7×10^5 cells/mL in 0.9%

(v/v) NaCl solution), while the lower chambers were filled with 400 μL of physiological solution containing the peptide. A polycarbonate membrane (10 μm pore diameter, NeuroProbe, USA) was placed between the two chambers. The chemotaxis chamber was incubated at 37 °C for 1 h. After incubation, the cells in the lower chambers were counted using a Neübauer chamber. The results were expressed as the number of migrating cells/mL and are reported as an average (±SD). The peptide Protonectin 1-6 was used as standard compound for positive control of this assay.

von Frey electronic pressure-meter paw tests for mice

Hyperalgesia was induced by intraplantar (i.pl.) injection of carrageenan (300 μg) or Secapin-2 (1, 2, 4, 10, 30 and 50 μg) into one of the hind paws. The mice were placed in acrylic cages (12 cm × 10 cm × 17 cm high) with a wire grid floor 15–30 min before testing. During this adaptation period, the paws were poked 2–3 times. Before paw stimulation, the animals were quiet, lacked exploratory movements and defecation, and were not resting on their paws. In these experiments, we used a pressure-meter that consisted of a hand-held force transducer fitted with a 0.5 mm^2 polypropylene tip (electronic von Frey anesthesiometer, IITC Inc., Life Science Instruments, Woodland Hills, CA, USA). The investigator was trained to apply the polypropylene tip perpendicularly to the central area of the hindpaw with a gradual increase in pressure. A tilted mirror below the grid provided a clear view of the animal's hindpaw. The test consisted of poking a hindpaw to provoke a flexion reflex followed by a clear flinch response after paw withdrawal. In the electronic pressure-meter test, the intensity of the stimulus was automatically recorded when the paw was withdrawn. The maximal force applied was 18 g. The stimulation of the paw was repeated until the animal presented two similar measurements. If the results were inconsistent (i.e., a great difference was observed in the baseline response compared to the other animals in the experiment), another animal was used. The results are reported as the Δ (delta) withdrawal threshold (g), which was calculated by subtracting the values obtained after the treatment from the first measurement (before the treatment).

Evaluation of edema

Edema was induced by the i.pl. injection of carrageenan (300 μg) or Secapin-2 (1, 2, 4, 10, 30 and 50 μg) into one of the hind paws. The thickness increase (edema) of the paws up to the tibio-tarsal articulation was measured using a digital pachymeter (Mitutoyo, CD-6″ CSX-B model, Brazil). The difference between the values obtained for both paws expressed as the percent increase in paw thickness was used as a measure of edema.

To evaluate the nociceptive activity of Secapin-2, the peptide was dissolved in sterile saline (0.005, 0.35, 1, 2, 10 and 30 μg) and administered by i.pl. injection into one of the hind paws of the mice. A hypodermic 26-G needle was inserted into the skin of the second footpad (to avoid back flow), and the tip of the needle was introduced into the central area of the hindpaw in the same place where the filaments or the tip of the pressure-meter were applied. The nociceptive activity was evaluated at different times (0-before the treatment, 15, 30, 60, 120, 180, 240, 360, 480 and 1440 min) after treatment and compared to the control. Carrageenan (Marine Colloids, 300 μg) was diluted in sterile saline and was used as a positive control. Sterile saline was used as a control. To evaluate the role of prostanoids in the hyperalgesia and edema induced by crude bee venom, the cyclooxygenase inhibitor Indomethacin was used. Indomethacin (Sigma, USA, 100 μg) or 0.1 M Tris–HCl buffer, pH 8.0 (control) was administered by i.pl. injection to the mice 30 min before the peptide inoculation [9]. To evaluate the involvement of lipid mediators in the peptide-induced hyperalgesia, Zileuton (Abbott Laboratories, Zyflo®, USA) (100 mg/kg, administered orally), a lipoxygenase inhibitor, were administered 60 min before injection of the peptides. The Zileuton was diluted in a solution of 10% (v/v) ethyl-alcohol. Animals injected with 10% (v/v) ethyl-alcohol solution plus sterile saline were used as the control group. To evaluate the involvement of leukotriene receptors, Zafirlukast (Sigma, USA) (5.0 mg/kg, administered orally) was diluted in 0.5% dimethyl sulfoxide (DMSO, Sigma, USA).

Statistical analysis

Two-way analysis of variance (ANOVA) was used to compare the groups and doses over all the time points. The factors analyzed were the treatments, time and the time versus treatment interaction. When a significant time versus treatment interaction was detected, one-way ANOVA followed by the Tukey test was performed for each time point to distinguish the dose effects. One-way ANOVA followed by the Tukey test was also used for dose–response curves at a single time point. Results with $p < 0.05$ were considered significant.

Results

Structural characterization

The peptide fraction from Africanized honeybee venom (3.5 mg) was fractionated by reverse-phase HPLC, resulting in the elution of sixteen fractions (designated 1–16 in Fig. 1A). Fractions 1 and 2 consisted of histamine and serotonin, respectively (based on chromatograms developed in presence of standard compounds; not shown results); fractions 4–6 and 8–10 were determined to be very low abundant venom components not yet characterized, while fractions 11 and 14 corresponded to Apamin and Melittin, respectively (based on chromatograms developed in presence of standard compounds; not shown results). The peptide component of fraction 7 (empty arrow, Fig. 1A) was subjected to mass spectrometric analysis revealing an ESI mass spectrum characterized by the molecular ions of m/z 719.14 as $[M+H]^{+4}$, and m/z 958.52 as $[M+H]^{+3}$ (Fig. 1B). Fig. 1C shows the envelope of peaks at monoisotopic resolution for the quasi-molecular ion at m/z 719.14 as $[M+H]^{+4}$; the transformation of these data revealed that the peptide component of fraction 7 has a molecular mass of 2872.58 Da in the oxidized form (Fig. 1C). Considering that the mass spectrum indicated that the peptide component was highly pure, it was subjected to amino acid sequencing using automated Edman degradation chemistry, which revealed the following sequence: YIIDVPPRCPPGSKFVHKRCRVIVP.

The sequence of this peptide revealed the presence of two cysteine residues, which raised the possibility of a disulfide bridge formed by the thiol groups of the cysteine side chains under natural conditions. To test this possibility, the peptide was reduced by dithiothreitol treatment, and the mass spectra was reacquired, revealing a molecular of 2874.58 Da (data not shown), due to the incorporation of two hydrogens (one for each thiol group); this result confirms the existence of a disulfide bridge between the two cysteine residues. The molecular mass of 2874.58 Da for the natural peptide in its reduced form is consistent with an amidated C-terminal residue and the presence of an intramolecular disulfide bond; the complete primary structure of the peptide is shown in Fig. 1D.

Because the secondary structure is important for understanding the biological activities of the peptide, it was initially investigated using CD spectroscopy. The CD spectra of the oxidized form of the fraction 7 peptide obtained in water, in 40% (v/v) TFE, and in the presence of SDS below and above the CMC (at 165 μM and 8 mM SDS, respectively) are shown in Fig. 2.

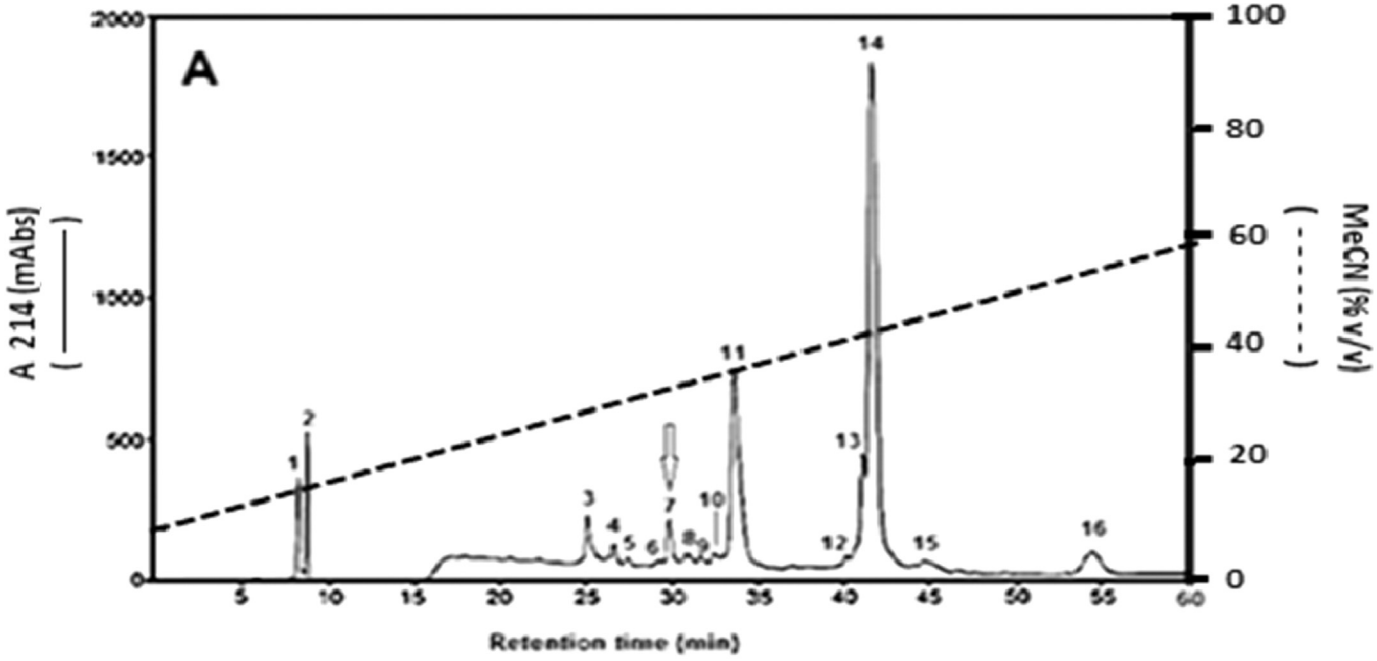

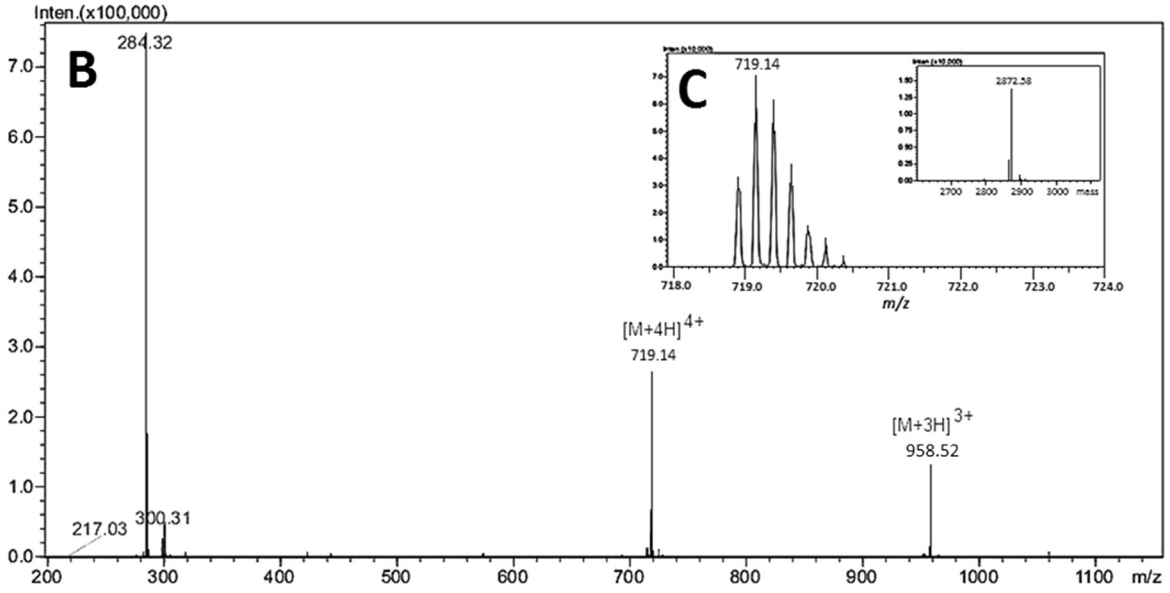

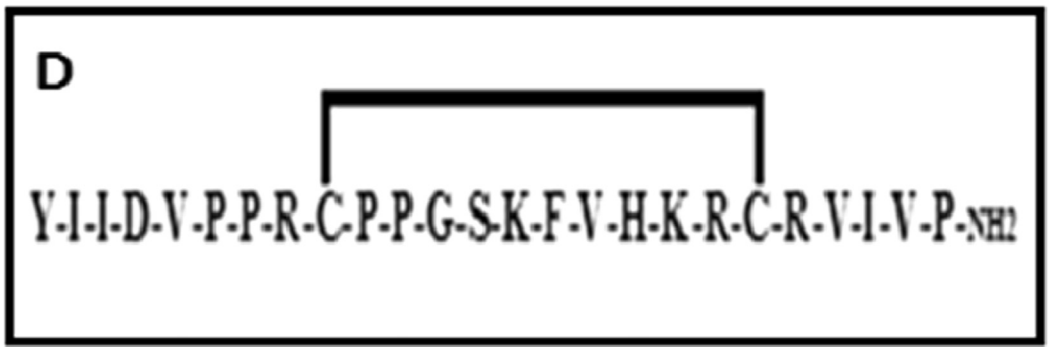

Fig. 1. (A) Chromatography profile of the peptide fractions of venom from Africanized *A. mellifera* under RP-HPLC using a Capcell Pack C-18 UG120 column (10 mm × 250 mm, 5 μm, Shisheido) under a linear gradient from 5 to 60% (v/v) MeCN/H_2O [containing 0.1% (v/v) TFA] at a flow rate of 2.0 mL/min for 60 min and monitored by UV absorption at 214 nm with a UV-DAD detector (Shimadzu, mod. SPD-M10A). The fractions were manually collected in glass vials and dried using a lyophilizer. The elution was monitored by measurement of the UV absorption at UV 214 nm. Fraction 7, containing the Secapin-2 peptide, is designated by an empty arrow. (B) ESI mass spectrum obtained in the positive mode for fraction 7; the peptide was detected as molecular ions of *m*/*z* 719.14 as $[M+H]^{+4}$, and *m*/*z* 958.52 as $[M+H]^{+3}$. (C) The insert is showing the envelope of peaks of the molecular ion at *m*/*z* 719.14 with monoisotopic resolution, and the transformation of the ESI/MS data revealing that the peptide has a molecular mass of 2872.58 Da in its oxidized form. (D) Amino acid sequence of Secapin-2 isolated from the venom of Africanized *A. mellifera* showing the connectivity of the disulfide bridge.

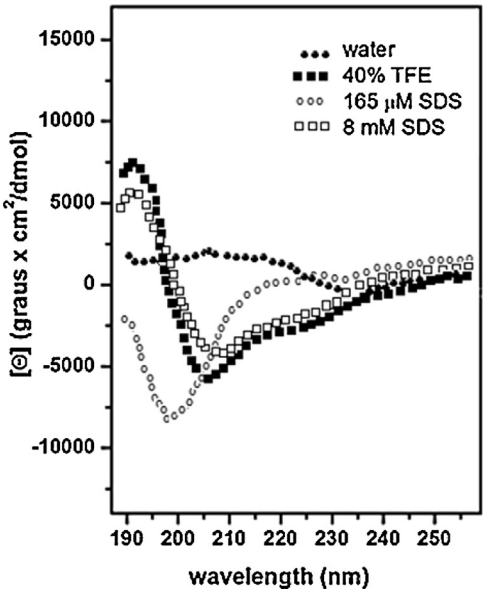

Fig. 2. CD spectra of Secapin obtained at 20 μM at 25 °C in the presence of water, 8 mM SDS and 40% (v/v) TFE. No smoothing has been applied.

The spectrum of the peptide in water (Fig. 2) is characteristic of an unordered conformation. In a medium composed of 40% (v/v) TFE and also in 8 mM SDS, two negative dichroic bands were observed, which is consistent with the induction of some α-helical conformations under these conditions. Nevertheless, the two negative dichroic bands observed for the fraction 7 peptide (208 and 222 nm) are characteristic of an α-helix. SDS below the CMC tends to induce β-sheet conformations and mimics the core environment of proteins [6]. Sequences with either lower helical propensities or which show a tendency to form aggregates will deviate from the helical pattern. The CD spectrum obtained in this environment clearly indicated that the fraction 7 peptide has reduced helical content. Table 1 shows the molar ellipticity ($[\Theta_{222}]$) and the α-helical fraction (f_H*) calculated according to the two-state model [40]. In addition, the CD spectra, in different environments, were analyzed by spectral deconvolution using the CONTIN program and the protein database SMP56 within the CDPro package. The analyses showed slightly higher helical contents (regular and distorted α-helical content) compared to those obtained with the two-state model. These analyses also showed that the peptide possesses many unordered and turn structures.

The molecular model of the fraction 7 peptide is shown in Fig. 3; the analysis of the Ramachandran plot for this molecular model (Fig. 1 in supplementary content) revealed that more than 90% of the residues lie in the most favorable regions. These results indicate that the model is adequate for structural studies. The molecular model of the peptide possesses a small helix that is maintained and most likely stabilized by the disulfide bridge (Fig. 3).

Table 1
Secondary structure evaluation of Secapin in different environments: water, 40% (v/v) TFE solution, 165 μM SDS, and 8 mM SDS Molar ellipticity ($[\Theta]_{222}$) and α-helix fractions (f_H*) were calculated according to the two-state model [40], and the fraction content of helical (H), strand (S) and unordered (Unrd) structures were obtained from the spectral deconvolution using the package CDPro (CONTIN, SMP56).

Condition	$[\Theta]_{222}$	f_H*	H	S	Unrd
Water	1260 ± 38	rc	-	-	-
40% (v/v) TFE	-3350 ± 68	0.12	0.15	0.37	0.39
165 μM SDS	-124 ± 75	-	0.03	0.45	0.22
8 mM SDS	-2460 ± 37	0.11	0.14	0.21	0.27

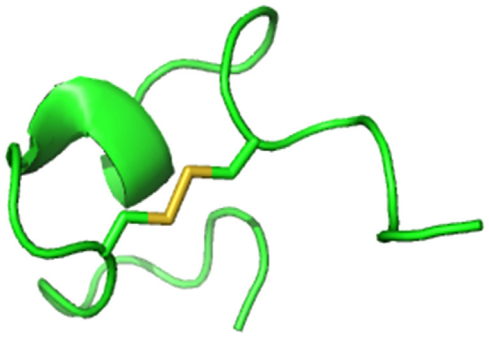

Fig. 3. Representation of the 3-D model of the Secapin-2 peptide.

Despite the fact that the molecular model is considered adequate by the criteria considered above, it is a static model. To obtain a more realistic idea of the structure of this peptide, the model above was subjected to molecular dynamics (MD) analysis. The purpose of performing molecular dynamics was to investigate the stability of the secondary structure of the peptide; this analysis was performed by evaluating different variables:

(i) The root-mean-square deviation (RMSD) of the positions for all backbone C-α atoms as a function of simulation time (Fig. 4A). The RMSD values for the C-α atoms of the peptide initially increased rapidly during the MD simulation (until 8000 ps). However, this increase was followed by a period of relative stability for most of the remaining simulation time. The RMSD values for the C-α atoms of the peptide remained stable throughout the MD simulation, suggesting that 20 ns of unrestrained simulation were sufficient to stabilize the peptide.
(ii) The radius of gyration is the root-mean-square distance of the atoms in relation to the *x*, *y* and *z* axes of a specific molecule, and it can be indicative of the size and compactness of a molecule. Fig. 4B shows that the peptide had a radius of gyration of 0.95 nm after 20 ns simulation. These results indicate that the presence of the disulfide bridge stabilizes the peptide into a compact molecular structure.
(iii) Analysis of the potential energy (Fig. 4C) shows that the peptide reached equilibrium and did not exhibit any asymptotic behavior.

The surface charge representation of the peptide (Fig. 5) shows that it has a compact structure characterized by two surfaces presenting a central region of positive residues that is located between two opposite regions of negative charge.

Functional characterization

Because nothing is known about the pharmacological and physiological effects of the fraction 7 peptide present in the crude venom of *A. mellifera*, one of the goals of the present investigation was to determine whether this peptide exhibits some of the biological activities typical of the polycationic peptides from Hymenoptera venoms. To this end, the peptide was assayed for mast cell degranulation, hemolysis, and chemotaxis of PMLNs but did not exhibit any of these activities (Figs. 2–4 in Supplementary content).

Another objective of the present study was to investigate the involvement of this peptide in the induction of the hyperalgesia/analgesia and inflammation/anti-inflammation processes. For this purpose, different doses of Secapin (0.005, 0.35, 1, 2, 10 and 30 μg) were injected into mice by intraplantar (i.pl.) administration, and the mice were tested for mechanical hyperalgesia (through the electronic von Frey) at different times (15, 30, 60, 120, 180, 240, 360, 480 and 1440 min) after the peptide administration.

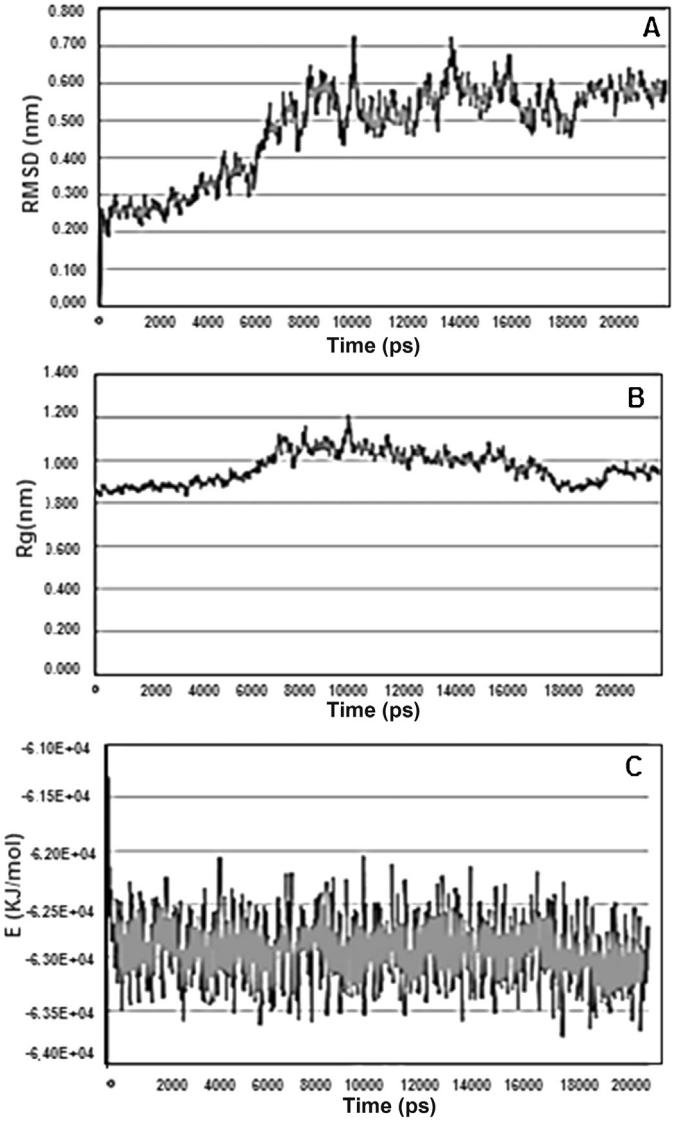

Fig. 4. Molecular dynamics simulations of Secapin. (A) Root mean-square deviation (RMSD), (B) radius of gyration (Rg), and (C) potential energy.

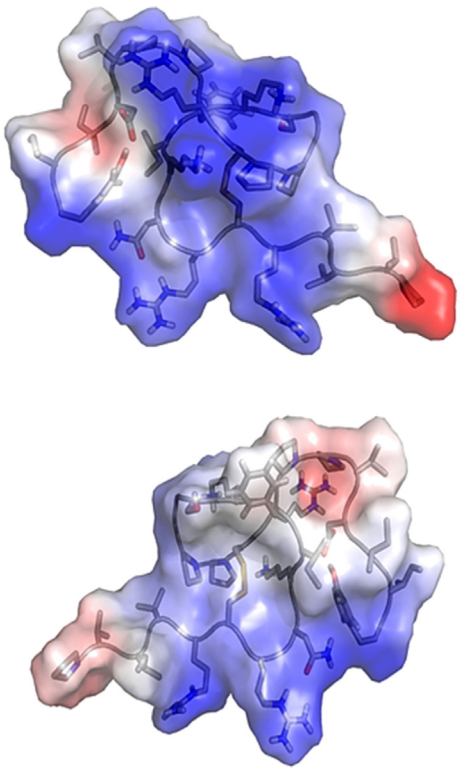

Fig. 5. Structural model of Secapin-2 as a charge surface representation in two different molecular surfaces. Negative residues are shown in dark gray (red in the web version), and positive residues are shown in gray (blue in the web version), hydrophilic in light gray and hydrophobic in white.

The control group animals were injected with the same vehicle (saline – S) that was used to dilute the peptide under the same experimental conditions. The positive control animals received i.pl. injection of carrageenan (Cg) at a dose of 300 μg.

The results show that in the first 15 min after the injection of the fraction 7 peptide there was a significant peak of pain (higher than that caused by the carrageenan); after this time, a decrease in pain threshold was observed, which was characterized as hypernociception (hyperalgesia) (Fig. 6A, C and E). However, this hyperalgesia persisted for 1440 min when the peptide dose was 10 or 30 μg (Fig. 6A), 480 min when it was 1, 2, 0.005 or 0.35 μg (Fig. 6C and E). The animals treated with carrageenan (positive control) exhibited a hyperalgesic effect for more than 1440 min (Fig. 6A, C and E). In addition, no significant differences were observed in the nociceptive threshold of the control group animals (Fig. 6A, C and E).

In addition to hyperalgesia, the edema activity of the peptide was also evaluated. The results showed that 10 or 30 μg of the peptide induced a significant increase in paw thickness (compared with carrageenan) from 15 to 30 min after the peptide injection; after 30 min, the edema decreased continuously up to 240 min (Fig. 6B). The paw thickness induced by peptide doses between 2 and 0.005 μg was lower than that induced by carrageenan, and decreased slowly until 240 or 360 min, depending on the peptide dose (Fig. 6C and F).

Because the peptide induced hyperalgesia and edema effects, the next objective was to investigate the involvement of prostanoids and lipid mediators derived from the cyclooxygenase and lipoxygenase pathways, respectively, in these effects. Mice were injected with the fraction 7 peptide (0.35 μg i.pl.) and treated with Indomethacin (Indo, 100 μg i.pl.), a cyclooxygenase pathway inhibitor, or Zileuton (Zil, 100 mg/kg orally in 500 μL), a lipoxygenase pathway inhibitor, and were tested for mechanical hyperalgesia and edema formation.

The results showed that Zileuton suppressed the peptide-induced hyperalgesia at 15 and 60 min when compared with the control group. On the other hand, Indomethacin did not suppress this effect (Fig. 7A and C).

Zileuton also suppressed the peptide-induced edema; however, only partial suppression was observed 15 min after administration of the peptide, while complete suppression was observed 60 min after peptide administration (Fig. 7B and D). On the other hand, Indomethacin did not suppress the edema, which was not significantly different in treated animals compared with the control group.

Because the results presented here showed that Zileuton suppressed the peptide-induced hyperalgesia and edema, it became important to study further the mechanisms of action induced by this peptide. For this purpose, Zafirlukast, a leukotriene receptor antagonist, was injected into mice (5 mg/kg in 300 μL of 0.5% (v/v) DMSO orally). The results indicated that Zafirlukast partially blocked the hypernociceptive effect of the peptide 15 min after peptide administration when compared with the control group (Sec + S) (Fig. 8A). The group treated with 0.5% (v/v) DMSO vehicle (DMSO + Sec) showed no difference from the control group (Sec + S) (Fig. 8A). Zafirlukast also partially inhibited the edema thickness

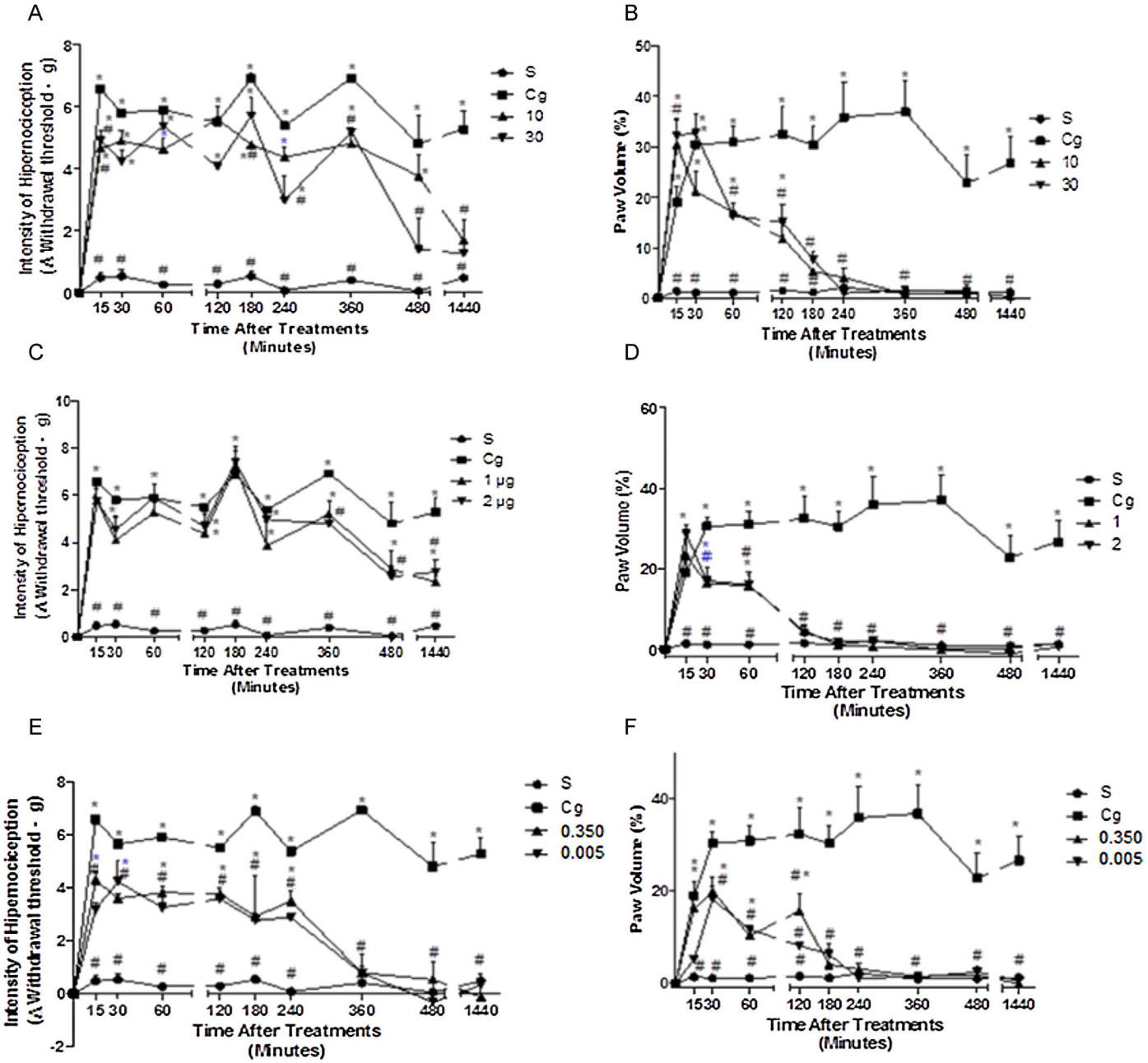

Fig. 6. Evaluation of the hyperalgesic and edematogenic effects of Secapin-2. The paw threshold was estimated using an electronic von Frey device. The force needed to induce paw withdrawal was recorded as the pain threshold represented by delta (Δ) (A, C, and E). Edematogenic effects were evaluated using a digital caliper pachymeter (B, D, and F). The data were obtained at time 0 and at 15, 30, 60, 120, 180, 240, 360, 480 and 1440 min after Secapin-2 administration (10 and 30 μg i.pl. shown in A and B, 1 and 2 μg i.pl. shown in C and D, and 0.35 and 0.005 μg i.pl. shown in E and F) or carrageenan administration (Cg, 300 μg i.pl.). The control group consisted of animals injected with sterile saline (S). The results are expressed as the mean ± SEM of 5 animals per group. $^{*}p < 0.001$, a significant difference compared with the mean values of the saline (S) group; $^{\#}p < 0.001$, a significant difference compared with the mean values of the carrageenan (Cg) group.

(Fig. 8A). The group treated with 0.5% (v/v) DMSO (Sec + DMSO) showed no significant difference from the control group (Sec + S) (Fig. 8B).

Discussion

The peptide purified from fraction 7 of the Africanized honeybee venom had a sequence (YIIDVPPRCPPGSKFVHKRCRVIVP-NH2) very similar to that of Secapin, which was originally isolated from a European species of *A. mellifera* (YIIDVPPRCPPGSKFIKNRCRVIVP-NH2) [35,49] and related to a variant form of this peptide isolated from the venom of *A. mellifera* in China named Secapin-1 (YIINVPPRCPPGSKFVKNKCRVIVP-NH2) [37]; therefore, the peptide isolated from fraction 7 was designated Secapin-2.

The polymorphic changes observed between Secapin-2 and Secapin included substitutions at amino acids 16–18, while the differences between Secapin-1 and -2 were substitutions at 17–19. All of these different forms of Secapin shared a disulfide bridge between the Cys 9 and Cys 20 residues.

The secondary structure of Secapin-2 was investigated by CD spectroscopy; apparently, this peptide has reduced helical content in anisotropic and membrane-mimetic environments. This analysis also showed that Secapin-2 has relatively high strand structure content. A structurally reliable molecular model was developed using

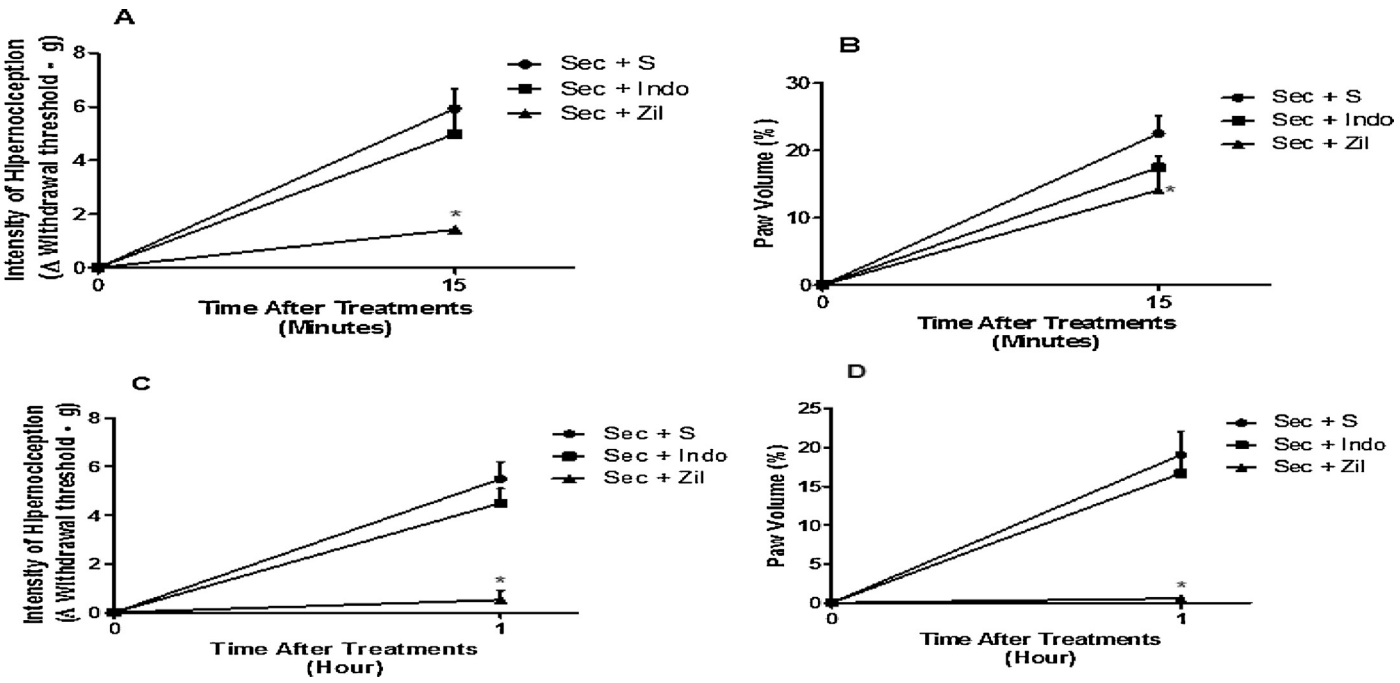

Fig. 7. Involvement of eicosanoids in the hyperalgesic and edematogenic effects of Secapin-2. The paw threshold was estimated using an electronic von Frey device. The force needed to induce paw withdrawal was recorded as the pain threshold represented by delta (Δ) (A and C). Edematogenic effects were evaluated using a digital pachymeter (B and D). The data were obtained at time 0, 15 min (A and B) and 1 h (C and D) after Secapin-2 administration (30 μg i.pl.). Indomethacin (I, 100 μg i.pl.) and Zileuton (Z, 100 mg/kg, orally in 500 μL) were administered 30 min and 1 h before peptide injection, respectively. The control group consisted of animals injected with Secapin-2/Saline. The results are expressed as the mean ± SEM of five animals per group. $^*p < 0.001$, a significant difference compared with the mean values of the Secapin-2/Saline group.

algorithms of structural biology and molecular dynamics; accordingly, the structure of Secapin-2 appears to be compact, stable, and stabilized by the disulfide bridge. A careful observation of this model revealed that the molecule has two easily distinguishable surfaces (Fig. 5), which are characterized by positive charges at the center of these surfaces that are flanked by two small regions of negative charge.

A structural comparison between the secondary structures of the peptides Apamin, Tertiapin and Secapin, which were isolated from honeybee venom, showed that these peptides have a common structural motif that is composed of a β-turn covalently linked to a short α-helical segment by one disulfide bond. Apamin and Tertiapin have two copies of this motif as both peptides have two intramolecular disulfide bridges [28]. The molecular model developed in the present study also shows this motif (Fig. 3).

Some studies have reported different activities than those found for Secapin for *A. mellifera* crude venom and/or some of the peptide toxins isolated from this venom [10,44].

Lariviere and Melzack [32] published the first experimental data using *A. mellifera* crude venom in an animal model, demonstrating that the nociceptive activity of this venom was dose dependent and lasted up to 60 min. Chen et al. [10] also reported a hyperalgesic effect caused by bee venom when injected into the hind paw of rats, reporting that this effect may be different depending on the noxious stimulus used. For example, mechanical stimulus caused a drop of 48% in the nociceptive threshold of the animal, while thermal stimulus caused a drop of 42% in this threshold. Importantly, this study also reported that the hyperalgesic effect was long lasting because 0.2 mg of the crude venom caused hyperalgesia that lasted for 3 days.

Brigatte et al. [8] studied the hyperalgesic and edematogenic effects of Melittin using a mechanical stimulus (electronic von Frey) in mice. This study reported that the hyperalgesic effect persisted for more than 8 h after administration for all peptide doses assayed, while the edema was long lasting only at high doses of Melittin.

In the present study, the duration of the hyperalgesia and edema were evaluated; the hyperalgesic effect persisted for up to 24 h at doses of 1 and 2 μg, while the effect lasted only up to 8 h at doses of 10 and 30 μg. These results are similar to those previously reported for Melittin [8]. The edematogenic effect was significantly different in the treated groups compared with the control group, persisting longer than 19 h at doses of 30 and 50 μg Secapin-2.

Once the effect of Secapin-2 was characterized by the occurrence of hyperalgesia and edema, the next step was to evaluate the chemical mediators involved in these processes. For this purpose, animals were treated with Indomethacin and Zileuton (nonspecific antagonists of cyclooxygenase and lipoxygenase, respectively).

The results of the present study showed a partial suppression of hyperalgesia and edema in the animals treated with Zileuton 15 min after Secapin-2 injection and complete suppression 60 min after peptide injection. The animals treated with Indomethacin showed no significant effect compared with the control group.

Like Secapin-2, Melittin-induced hyperalgesic and edematogenic effects were previously reported to involve lipid mediators [8]. On the other hand, prostanoids were shown to mediate the pain and inflammation induced by crude bee venom because Indomethacin reversed these effects [33].

After observing that Zileuton reversed the hyperalgesia and edema induced by Secapin-2, the next step was to assay the ability of Zafirlukast to suppress pain and edema. As observed for Zileuton, Zafirlukast partially reversed the actions induced by Secapin-2, indicating that leukotriene receptors must mediate the action of this peptide.

Taken together, these data showed that Secapin-2 does not induce hemolytic activity, mast cell degranulation, or PMNL chemotaxis; however, it does induce hyperalgesia and edema mediated by leukotrienes. In comparison, the peptide Paulistine was recently reported; this peptide was isolated from the venom of the social wasp *P. paulista*, had a structural motif similar to that described above for Secapin-2, and caused hyperalgesia

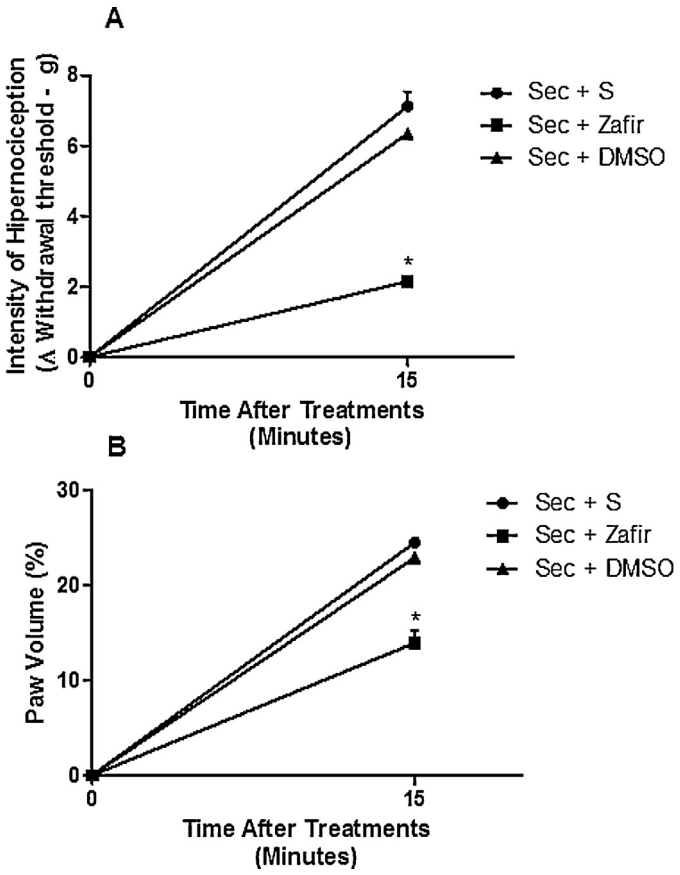

Fig. 8. Involvement of leukotriene receptors on the hyperalgesic and edematogenic effects of Secapin-2. The paw threshold was estimated using an electronic von Frey device. The force needed to induce paw withdrawal was recorded as the pain threshold represented by delta (Δ) (A). Edematogenic effects were evaluated using a digital pachymeter (B). The data were obtained at time 0, and 15 min after Secapin-2 administration (30 μg i.pl.). Zafirlukast (Zafir, 5 mg/kg, orally), an antagonist of the leukotriene receptor, was administered before Secapin-2 administration (Sec + Zafir). The reference groups consisted of animals injected with Secapin-2/saline and Secapin-2/DMSO. The results are expressed as the mean ± SEM of five animals per group. $^{*}p < 0.001$, a significant difference compared with the mean values of the Secapin-2/saline and Secapin-2/DMSO groups.

by interacting with the receptors of lipid mediators involved in the cyclooxygenase type II pathway [26]. The mechanism of action of Secapin-2 on leukotrienes pathway is unknown, but taking into account of the inhibitory effects of Zileuton and Zafirlukast in the inflammatory action caused by the peptide, it may be considered that: (i) Zileuton is an inhibitor of the 5-lipoxygenase (5-LO), which catalyzes the first two catalytic steps of this pathway [52]; (ii) Zafirlukast blocks the action of the cysteinyl leukotrienes on CysLT1 receptors [53]; (iii) Therefore, the site(s) of interaction with Secapin-2 must located in the metabolic steps between the 5-LO and the CysLT1 receptors.

Conclusion

In conclusion, the present investigation led to a better understanding of the inflammation and pain induced by honeybee venom. Although the existence of the Secapin peptide (and its analogs) in honeybee venom has been known for approximately 38 years, almost nothing has been known about the pharmacology of this peptide until now. The present work has pioneered the functional characterization of this toxin and revealed that Secapin-2 induces inflammation and pain through the lipoxygenase pathway.

Conflict of interest

The authors have nothing to disclose. No conflict of interest exists.

Acknowledgement

This research is supported by grants from FAPESP (Proc. 04/07942-2, BIOprospecTA Proc. 2011/51684-1), CNPq and Instituto Nacional de Ciência e Tecnologia de Investigação em Imunologia-iii (INCT/CNPq-MCT). MSP and JRN are researchers for the Brazilian Council for Scientific and Technological Development (CNPq).

Appendix A. Supplementary data

Supplementary material related to this article can be found, in the online version, at http://dx.doi.org/10.1016/j.peptides.2014.07.004.

References

[1] Albericio F, Annis FI, Royo M, Barany G. Preparation and handling of peptides containing methionine and cysteine. In: Cheng C, White PD, editors. Fmoc solid phase peptide synthesis: a practical approach. Oxford, UK: Oxford University Press; 2004. p. 77–114.
[2] Altschul SF, MaddenTL, Schaffer AA, Zhang J, Zhang Z, Miller W, et al. Gapped BLAST and PSI-BLAST: a new generation of protein database search programs. Algorithm for rigid water models. J Comput Chem 1992;13:952–62.
[3] Banks BEC, Shipolini RA. Chemistry and pharmacology of honey bee venom. In: Piek T, editor. Venom of the Hymenoptera: biochemical, pharmacological and behavioral aspects. London, UK: Academic Press; 1986. p. 329–415.
[4] Berendsen HJC, Postma JPM, van Gunsteren WF, DiNola A, Haak JR. Molecular dynamics with coupling to an external bath. J Chem Phys 1984;81:3684–90.
[5] Berman HM, Westbrook J, Feng Z, Gilliland G, Weissig TN, Shindyalov H, et al. The protein data bank. Nucleic Acids Res 2000;28:235–42.
[6] Blondelle SE, Forood B, Houghten RA, Perez-Paya E. Secondary structure induction in aqueous vs membrane-like environments. Biopolymers 1997;42:489–98.
[7] Breithaupt H, Habbermann E. Mast zell degranulierendes Peptide (MAD-Peptide) aus bienegift: isolierun, biochemische und pharmakologische eigenschaften. Naunyn Schimiedebergs Arch Exp Pathol Pharmakol 1968;261:252–70.
[8] Brigatte P, Cury Y, De Souza BM, Baptista-Saidemberg NB, Saidemberg DM, Gutierrez VP, et al. Hyperalgesic and edematogenic effects of peptides isolated from the venoms of honeybee (*Apis mellifera*) and neotropical social wasps (*Polybia paulista* and *Protonectarina sylveirae*). Amino Acids 2011;40:101–11.
[9] Chacur M, Longo I, Picolo G, Gutierrez JM, Lomonte B, Guerra JL, et al. Hyperalgesia induced by Asp49 and Lys49 phospholipases A_2 from *Bothrops asper* snake venom: pharmacological mediation and molecular determinants. Toxicon 2003;41:667–78.
[10] Chen J, Luo C, Li HL, Chen HS. Primary hyperalgesia to mechanical and heat stimuli following subcutaneous bee venom injection into the plantar surface of hindpaw in the conscious rat: a comparative study with the formalin test. Pain 1999;83:67–76.
[11] Chen J, Lariviere WR. The nociceptive and anti-nociceptive effects of bee venom injection and therapy: a double-edge sword. Prog Neurobiol 2010;92:151–83.
[12] Chowdhuri S, Tan ML, Ichiye T. Dynamical properties of the soft sticky dipole-quadrupole-octupole water model: a molecular dynamics study. J Chem Phys 2006;125:144513.
[13] Corzo G, Bernard C, Clement H, Villegas E, Bosmans F, Tytgat J, et al. Insecticidal peptides from the theraposid spider *Brachypelma albiceps*: an NMR-based model of Ba2. Biochim Biophys Acta 2009;1794:1190–6.
[14] De Graaf DC, Alerts M, Danneels E, Devreese B. Bee, wasp and ant venomics pave the way for a component resolved diagnosis of sting allergy. J Proteom 2009;72:145–54.
[15] Delano WL. The PyMOL Molecular Graphics System. San Carlos, CA, USA: DeLano Scientific; 2002. Available from <http://www.pymol.org>.
[16] De Souza BM, Mendes MA, Santos LD, Marques MR, César LMM, Almeida RNA, et al. Structural and functional characterization of two novel peptide toxins isolated from the venom of the social wasp *Polybia paulista*. Peptides 2005;26:2157–64.
[17] De Souza BM, Palma MS. Peptides from hymenoptera venoms: biochemistry, pharmacology and potential applications in health and biotechnology. In: DeLima ME, Pimenta AMC, Martin-Euclaire MF, Zingali RB, editors. Animal

toxins: the state of art – perspectives on health and biotechnology. Belo Horizonte: Editora UFMG; 2009. p. 273–97.
[18] De Souza BM, Silva AVR, Resende VMF, Arcuri HA, Dos Santos Cabrera MP, Ruggiero Neto J, et al. Characterization of two novel polyfunctional mastoparan peptides from the venom of the social wasp *Polybia paulista*. Peptides 2009;3:1387–95.
[19] Dias NB, De Souza BM, Gomes PC, Palma MS. Peptide diversity in the venom of the social wasp *Polybia paulista* (Hymenoptera): a comparison of the intra- and inter-colony compositions. Peptides 2014;51:122–30.
[20] Essmann U, Perera ML, Berkowitz ML, Darden T, Lee H, Pedersen LG. A smooth particle mesh Ewald method. J Chem Phys 1995;103:8577–93.
[21] Fioroni M, Burger K, Mark AE, Roccatano D. A model of 1,1,1,3,3,3-hexafluoropropan-2-ol for molecular dynamics simulations. J Phys Chem B 2001;105:10967–75.
[22] França FOS, Benvenuti LA, Fan HW, Dos Santos DR, Hain SH, Picchi-Martins FR, et al. Severe and fatal mass attacks by "killer" bees (Africanized honey bees – *Apis mellifera scutellata*) in Brazil: clinic-pathological studies with measurement in serum venom concentrations. Q J Med 1994;87:269–82.
[23] Gabriel DP, Rodrigues Jr AG, Barsante RC, dos Santos-Silva V, Caramori JT, Martim LC, et al. Severe acute renal failure after massive attack of Africanized bees. Nephrol Dial Transplant 2004;19:2680.
[24] Gauldie J, Hanson JM, Rumjanek FD, Shipolini RA, Vernon CA. The peptide components of bee venom. Eur J Biochem 1976;61:369–76.
[25] Gauldie J, Hanson JM, Shipolini R, Vernon CA. The structures of some peptides from bee venom. Eur J Biochem 1978;83:405–10.
[26] Gomes PC, De Souza BM, Dias NB, Brigatte P, Mourelle D, Arcuri HA, et al. Structure–function relationships of the peptide Paulistine: a novel toxin from the venom of the social wasp *Polybia paulista*. Biochim Biophys Acta 1840;1014:170–83.
[27] Miyamoto S, Kollman PA. SETTLE: an analytical version of the SHAKE and RATTLE algorithm for rigid water models. J Comput Chem 1992;13:952–62.
[28] Hider RC, Ragnarsson U. A comparative structural study of apamin and related bee venom peptides. Biochim Biophys Acta 1981;667:197–208.
[29] Humble Y, Sonnet J, de Strihou VYC. Bee stings and acute tubular necrosis. Nephron 1982;31:187–8.
[30] Konno T, Meguro H, Tuzimura K. D-Pantolactone as a circular dichroism calibration. Anal Biochem 1975;67:226–32.
[31] Konno K, Hisada M, Fontana R, Lorenzi CB, Naoki H, Itagaki Y, et al. Anoplin, a novel antimicrobial peptide from the venom of the solitary wasp *Anoplius samariensis*. Biochim Biophys Acta 2001;1550:70–80.
[32] Lariviere WR, Melzack R. The bee venom test: a new tonic-pain test. Pain 1996;66:271–7.
[33] Lariviere WR, Chesler EJ, Li Z, Shang GW, Chen YN, Yu YQ, et al. Correlations between edema and the immediate and prolonged painful consequences of inflammation: therapeutic implications? Sheng Li Xue Bao 2005;57:278–88.
[34] Laskowski RA, MacArthur MW, Moss DS, Thornton JM. PROCHECK: a program to check the stereochemical quality of protein structures. J Appl Cryst 1993;26:283–91.
[35] Liu LK, Vernon CA. The structure of secapin: a peptide from bee venom. J Chem Res 1984:10–1.
[36] Marti-Renom MA, Stuart AC, Fiser A, Sanchez R, Melo F, Sali A. Comparative protein structure modeling of genes and genomes. Ann Rev Biophys Biomol Struct 2000;29:291–325.
[37] Meng Y, Yang XX, Sheng YX, Zhang JL, Yu DQ. A novel peptide from *Apis mellifera* and solid-phase synthesis of its analogue. Chin Chem Lett 2012;23:1161–4.
[38] Neuman W, Habbermann E. Beiträge, zur characterisierumde Wirksstoffe des bienengiftes. Naunym-Chmiedebergs Arch Pahrmakol 1954;222:367–87.
[39] Palma MS. Hymenoptera venom peptides. In: Kastin A, editor. Handbook of biologically active peptides. 2nd ed. San Diego, USA: Academic Press; 2013. p. 416–22, 1942 pp. [Chapter 58].
[40] Rohl CA, Baldwin RL. Deciphering rules of helix stability in peptides. Meth Enzymol 1998;295:1–26.
[41] Sali A, Blundell TL. Comparative protein modelling by satisfaction of spatial restraints. J Mol Biol 1993;234:779–815.
[42] Scott WRP, Hunenberger PH, Tironi IG, Mark AE, Billeter SR, Fennen J, et al. The GROMOS biomolecular simulation program package. J Phys Chem A 1999;103:3596–607.
[43] Shen MY, Sali A. Statistical potential for assessment and prediction of protein structures. Prot Sci 2006;15:2507–24.
[44] Son DJ, Lee JW, Lee YH, Song HS, Lee CK, Hong JT. Therapeutic application of anti-arthritis, pain releasing, and anti-cancer effects of bee venom and its constituent compounds. Pharmacol Ther 2007;115:246–70.
[45] Spoerri PE, Jentsch J, Glees P. Apamin from honey bee venom: effects of the neurotoxin on cultures of the embryonic mouse cortex. Neurobiology 1972;3:207–14.
[46] Spoerri PE, Jentsch J, Glees P. Apamin from bee venom. Effects of the neurotoxin on subcellular particles of neural cultures. FEBS Lett 1975;53:142–7.
[47] Vick JA, Shipman WH, Brooks RB. Beta-adrenergic and anti-arrhythmic effects of cardioprep, a newly isolated substance from whole bee venom. Toxicon 1974;12:139–44.
[48] Van Der Spoel VD, Hess B, Groenhof G, Mark AE, Berendsen HJ. GROMACS: fast, flexible, and free. J Comput Chem 2005;26:1701–18.
[49] Vlasak R, Kreil G. Nucleotide sequence of cloned cDNAs coding for preprosecapin, a major product of queen-bee venom glands. Eur J Biochem 1984;145:279–82.
[50] Xu X, Nelson JW. Solution structure of tertiapin determined using nuclear magnetic resonance and distance geometry. Proteins 1993;17:124–37.
[51] Zimmermann M. Ethical guidelines for investigations of experimental pain in conscious animals. Pain 1983;16:109–10.
[52] Lu P, Schrag ML, Slaughter DE, Raab CE, Shou M, Rodrigues AD. Mechanism-based inhibition of human liver microsomal cytochrome P450 1A2 by zileuton, a 5-lipoxygenase inhibitor. Drug Metab Dispos 2003;31:1352–60.
[53] Fischer JD, Song MH, Suttle AB, Heizer WD, Burns CB, Vargo DL, et al. Comparison of Zafirlukast (Accolate) absorption after oral and colonic administration in humans. Pharmaceut Res 2000;17:154–9.